


Addendum to “Radiation emitted by a source orbiting a Schwarzschild–anti–de Sitter black hole”

João P. B. Brito^{*,} Rafael P. Bernar[†] and Luís C. B. Crispino[‡]

Programa de Pós-Graduação em Física, Universidade Federal do Pará, 66075-110 Belém, Pará, Brazil.

 (Received 1 September 2022; accepted 31 October 2022; published 15 November 2022)

In [J. P. B. Brito *et al.*, *Phys. Rev. D* **104**, 124085 (2021).], we studied the scalar radiation emitted by a source orbiting a Schwarzschild–anti–de Sitter black hole along circular geodesics. We presented results for the emitted power in the context of quantum field theory in curved spacetimes. We computed the emitted power for a region of the parameter space corresponding to large black holes when compared to the anti–de Sitter radius. In this addendum we investigate the regime of small black holes, i.e., the regime of $M^2\Lambda \lesssim 0$. In this regime, the emitted power, as a function of the source’s angular velocity, exhibits resonant peaks associated with quasinormal frequencies.

DOI: [10.1103/PhysRevD.106.104033](https://doi.org/10.1103/PhysRevD.106.104033)

In Ref. [1], we analyzed the scalar radiation emitted by a source moving along circular geodesics around a Schwarzschild–anti–de Sitter (SAdS) black hole. Using quantum field theory in curved spacetimes at tree level, we computed the partial and total emitted power by the source considering the family of SAdS black holes by varying the parameter $M^2\Lambda$. However, we restricted our attention to the region of the parameter space corresponding to $M^2\Lambda \leq -1/2$ (or equivalently $r_e > 0.6R_{\text{AdS}}$, where $R_{\text{AdS}} = \sqrt{3/|\Lambda|}$ is the anti–de Sitter radius). In this addendum, we present results for $M^2\Lambda \lesssim 0$ (or equivalently $r_e < 0.6R_{\text{AdS}}$).

For $M^2\Lambda \lesssim 0$, the effective potential for the scalar field presents a local maximum and a local minimum (see Fig. 1). The local minimum of the potential gives rise to long-lived modes [2–5], which lead to spikes in the total power emitted by the source, when plotted as a function of the source’s angular velocity. The spikes are located at values of the source’s angular velocity equal to the frequencies of the associated long-lived modes.

Although the dissipation at the horizon prevents the modes to be stationary, we can use the Bohr-Sommerfeld condition to obtain approximately the real part of the frequencies associated with these resonant modes. As was shown in Refs. [2,3], for small black holes the imaginary part of the quasinormal frequencies can be very small; i.e., the modes are long-lived¹ and are almost trapped inside the potential well present in $V_{\text{eff}}(r)$ [see Eq. (20) in Ref. [1]]. The potential V_{eff} is plotted in Fig. 1 for a

representative choice of $M^2\Lambda$ and l . The values of the characteristic energies (given by the square of the frequency) are shown as horizontal lines. These frequencies are obtained through the condition given by [2,3]

$$2 \int_{r_a}^{r_b} \frac{dr}{f_{\Lambda}(r)} \sqrt{\omega^2 - V_{\text{eff}}(r)} = (2n + 1)\pi, \quad (1)$$

with n being a non-negative integer number and r_a, r_b the classical turning points (see Fig. 1). We see that, the lower the value of n is, the closer the energies are to the minimum of the potential and therefore the associated modes should decay more slowly. For orbits far away from the photon

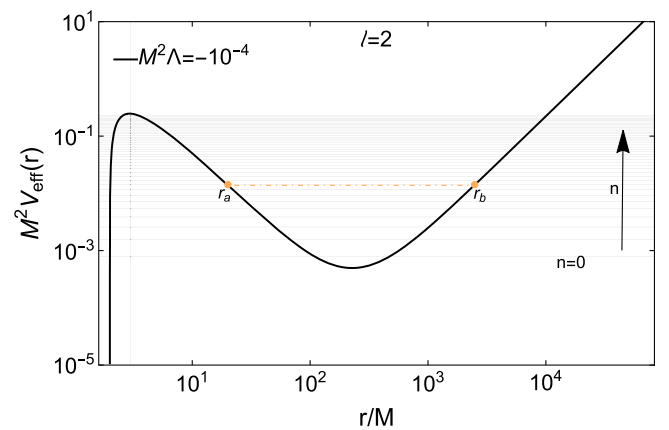


FIG. 1. The effective potential $M^2 V_{\text{eff}}$ defined in Eq. (20) of Ref. [1], with $l = 2$ for $M^2\Lambda = -10^{-4}$. The horizontal (gray) lines denote the energy levels associated with the resonant frequencies in the potential well and the vertical (gray) line marks the position of the photon sphere of the black hole ($r_0 = 3M$). The positions r_a and r_b are classical turning points.

*joao.brito@icen.ufpa.br

†rbernar@ufpa.br

‡crispino@ufpa.br

¹The damping timescale of these modes is proportional to r_e^{-2l-2} ; see Ref. [5]

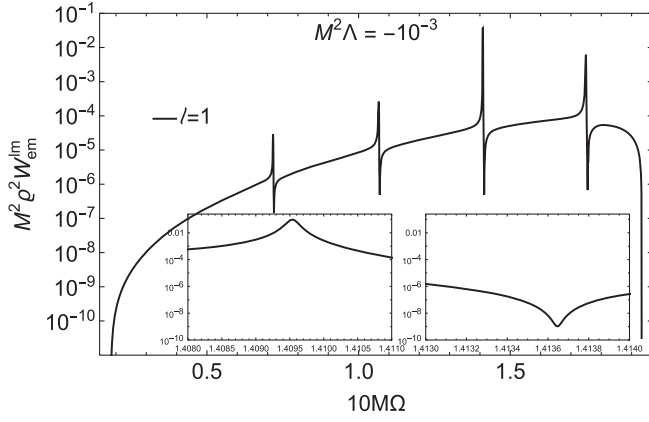


FIG. 2. The partial emitted power as a function of $M\Omega$ given by Eq. (47) of Ref. [1], for $M^2\Lambda = -10^{-3}$ and $l = 1$. The insets show in more details the third resonant pattern.

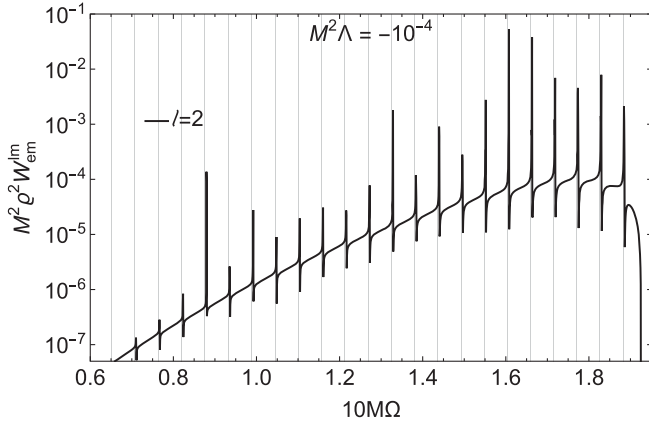


FIG. 3. The partial emitted power as a function of $M\Omega$ given by Eq. (47) of Ref. [1], for $M^2\Lambda = -10^{-4}$ and $l = 2$. The vertical (gray) lines denote the real part of the quasinormal frequencies.

sphere, the resonant frequencies approach the normal frequencies of the pure anti-de Sitter spacetime given by [2,6]

$$R_{\text{AdS}}\omega_{\text{AdS}} = 2n + l + 3. \quad (2)$$

In Fig. 2 we exhibit the partial emitted power in a log plot for a given value of $M^2\Lambda$, for which the resonant patterns are seen. The emitted power has sharp maximum and minimum in these locations, as shown by the insets.

In Fig. 3 we show the partial emitted power for a given value of $M^2\Lambda$ and l , with the resonant frequencies highlighted. We see that the real part of the quasinormal frequencies estimated by the Bohr-Sommerfeld condition (1) present excellent agreement with the resonant peaks of the partial power.

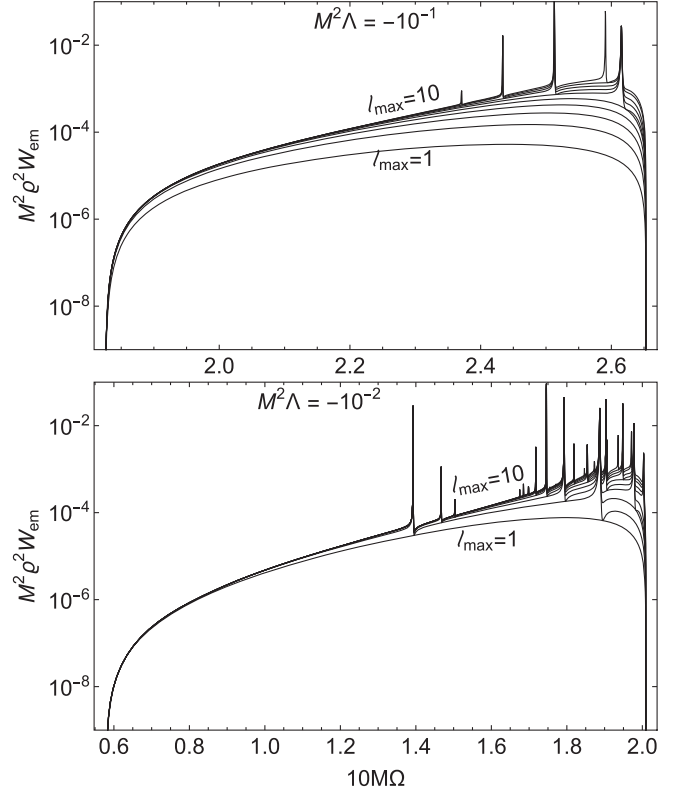


FIG. 4. The total emitted power as a function of $M\Omega$ given by Eq. (50) of Ref. [1], for $M^2\Lambda = -10^{-1}$ (top) and $M^2\Lambda = -10^{-2}$ (bottom) with different choices of l_{max} , up to $l_{\text{max}} = 10$, as indicated.

In Fig. 4, we plot the total emitted power by the source for two choices of $M^2\Lambda$. We see that the total power exhibits sharp peaks associated with the quasinormal frequencies presenting a distinctive characteristic of SAdS black holes with reflective boundary conditions at infinity (see Refs. [1,7–10] and the references therein). We can also see that the contribution of higher multipoles is important close to the photon sphere, i.e., for $\Omega \approx \Omega_{\text{max}}$. This is a feature of the scalar geodesic synchrotron radiation.

The authors thank Fundação Amazônia de Amparo a Estudos e Pesquisas, Conselho Nacional de Desenvolvimento Científico e Tecnológico, and Coordenação de Aperfeiçoamento de Pessoal de Nível Superior—Finance Code 001, in Brazil, for partial financial support. This work has been further supported by the European Union’s Horizon 2020 research and innovation program H2020-MSCA-RISE-2017 Grant No. FunFiCO-777740.

- [1] J. P. B. Brito, R. P. Bernar, and L. C. B. Crispino, Radiation emitted by a source orbiting a Schwarzschild–anti–de Sitter black hole, *Phys. Rev. D* **104**, 124085 (2021).
- [2] J. Grain and A. Barrau, A WKB approach to scalar fields dynamics in curved space-time, *Nucl. Phys.* **B742**, 253 (2006).
- [3] G. Festuccia and H. Liu, A Bohr-Sommerfeld quantization formula for quasinormal frequencies of AdS black holes, *Adv. Sci. Lett.* **2**, 221 (2009).
- [4] R. Daghigh and M. Green, A detailed analytic study of the asymptotic quasinormal modes of Schwarzschild–anti–de Sitter black holes, *Classical Quantum Gravity* **26**, 125017 (2009).
- [5] E. Berti, V. Cardoso, and P. Pani, Breit-Wigner resonances and the quasinormal modes of anti–de Sitter black holes, *Phys. Rev. D* **79**, 101501(R) (2009).
- [6] E. Berti, V. Cardoso, and A. O. Starinets, Quasinormal modes of black holes and black branes, *Classical Quantum Gravity* **26**, 163001 (2009).
- [7] L. C. B. Crispino, Synchrotron scalar radiation from a source in ultrarelativistic circular orbits around a Schwarzschild black hole, *Phys. Rev. D* **77**, 047503 (2008).
- [8] L. C. B. Crispino, A. R. R. da Silva, and G. E. A. Matsas, Scalar radiation emitted from a rotating source around a Reissner-Nordström black hole, *Phys. Rev. D* **79**, 024004 (2009).
- [9] C. F. B. Macedo, L. C. B. Crispino, and V. Cardoso, Semi-classical analysis of the scalar geodesic synchrotron radiation in Kerr spacetime, *Phys. Rev. D* **86**, 024002 (2012).
- [10] J. P. B. Brito, R. P. Bernar, and L. C. B. Crispino, Synchrotron geodesic radiation in Schwarzschild–de Sitter spacetime, *Phys. Rev. D* **101**, 124019 (2020).